Acta Cryst. (1996). D52, 966–972

Structure of Val122Ile Variant Transthyretin – a Cardiomyopathic Mutant

ANA M. DAMAS,[a,b]* SANDRA RIBEIRO,[a] VICTOR S. LAMZIN,[c] JOANA A. PALHA[a,b] AND MARIA J. SARAIVA[a,b]

[a]*Instituto de Ciências Biomédicas Abel Salazar, Universidade do Porto, Largo do Prof. Abel Salazar, No. 2, 4050 Porto, Portugal,* [b]*Centro de Estudos de Paramiloidose, Hospital de Sto. António, Porto, Portugal, and* [c]*European Molecular Biology Laboratory (EMBL), c/o DESY, Notkestrasse 85, 22603 Hamburg, Germany. E-mail: amdamas@ncc.up.pt*

(Received 23 November 1995; accepted 6 March 1996)

Abstract

The Val122Ile mutant transthyretin (TTR Ile122) is an amyloidogenic protein which has been described as the major protein component of amyloid fibrils isolated from patients with familial amyloidotic cardiomyopathy (FAC), a disease characterized by cardiac failure and amyloid deposits in the heart. The reasons for the deposition of TTR are still unknown and it is conceivable that a conformational alteration, resulting from the mutation, is fundamental for amyloid formation. The three-dimensional structure of TTR Ile122 was determined and refined to a crystallographic R factor of 15.8% at 1.9 Å resolution. The r.m.s. deviation from ideality in bond distances is 0.019 Å and in angle-bonded distances is 0.027 A. The presence of two crystallographically independent monomers in the asymmetric unit allowed additional means of estimation of atomic coordinate error. The structure of the mutant is essentially identical to that of the wild-type transthyretin (TTR). The largest deviations occur in surface loops and in the region of the substitution. The protein is a tetramer composed of identical subunits; each monomer has two four-stranded β-sheets which are extended to eight-stranded β-sheets when two monomers associate through hydrogen bonds forming a dimer, which is the crystallographic asymmetric unit. The replacement of valine for isoleucine introduces very small alterations in relation to the wild-type protein; nevertheless they seem to confirm a tendency for a less stable tetrameric structure. This would support the idea that the tetrameric structure might be disrupted in amyloid fibrils.

1. Introduction

Human transthyretin (TTR) is a plasma protein which is involved in the transport of thyroxin. It also binds retinol binding protein, the carrier for vitamin A. In 1984 a variant TTR (Val30Met) was described as the major component of the amyloidogenic material present in patients with familial amyloidotic polineuropathy (FAP) (Saraiva, Birken, Costa & Goodman, 1984). This disease, first described by Andrade (1952), is characterized by a lower limb neuropathy with the predominant involvement of the peripheral nervous system (Andrade, 1952; Andrade, Arakis & Block, 1970). Val122Ile mutant transthyretin also belongs to the class of amyloidogenic proteins. It is the major protein component of the amyloid fibrils isolated from patients with familial amyloidotic cardiomyopathy (FAC), a disease characterized by cardiac failure and amyloid deposited in the heart, which is found mostly in the black population (Gorevic, Prelli, Wright, Pras & Frangione, 1989).

Over the past few years several pathogenic and non-pathogenic mutations in the TTR protein have been described in the literature. Most of the pathogenic variants are related by amyloidosis, although the clinical symptoms vary among different variants. They include polyneuropathies, cardiac failure, vitreous problems and carpal tunnel syndrome (Saraiva, 1991, 1995). A point mutation, which occurs in different places in the polypeptide chain, is described for most of the variants.

The three-dimensional structure of wild-type TTR was determined by Blake (Blake, Geisow, Oatley, Rerat & Rerat, 1978), who described it as a tetrameric structure composed of four identical subunits, each of them with 127 amino acids. There is a channel running through the molecule in which two equivalent binding sites for thyroxin are located; the hormone interacts with the side chains of two monomers from different dimers. Fig. 1 shows the TTR tetramer viewed along the channel. For each monomer the location of amino acid Ile at position 122 is also shown. Recently the crystal structure of TTR complexed to retinol-binding protein (RBP) was reported (Monaco, Rizzi & Coda, 1995). The authors show the interaction of two RBP molecules with one TTR tetramer.

The reasons for the deposition of TTR in the extracellular tissues, particularly when the protein contains an amyloidogenic mutation, are still unknown. It is conceivable that a conformational alteration, because of the mutation, is the determinant for amyloid formation.

Analysis of the distribution of the amyloidogenic mutations in the TTR molecule revealed that they

occur mainly at the surface, although they are not confined to the same region of the molecule (Damas, Terry & Blake, 1990). Hamilton and co-workers have reported their X-ray crystallographic studies on TTR Val30Met isolated from a homozygous patient (Hamilton *et al.*, 1992, 1993). Their results show an increase in the unit-cell volume, which is consistent with elongation of hydrogen bonds between the dimers. They have also indicated the existence of structural differences between the wild-type and the mutant protein, but none of these variations was considered significant. X-ray crystallographic studies of recombinant Val30Met TTR were also reported (Terry *et al.*, 1993). A major alteration was the movement of strand *A* in order to accommodate the Met30 side chain.

In order to increase our knowledge about the amyloid process, we have determined the crystal structure of TTR Ile122, one of the most frequent mutations in cases involving cardiac failure. In this paper we report the three-dimensional structure of this mutant protein refined to 1.9 Å resolution and a comparison with the structure of the wild-type protein. Preliminary work has been reported in abstract form (Damas *et al.*, 1993).

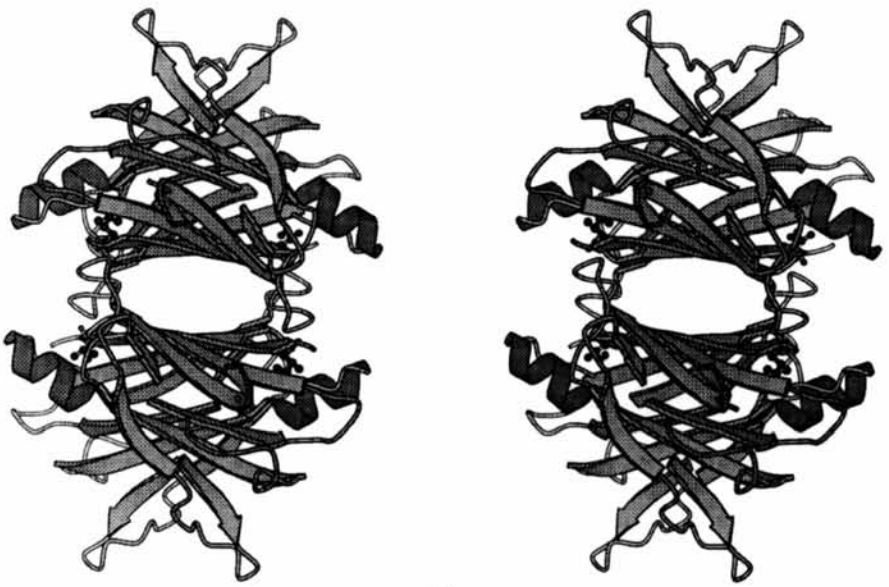

(*a*)

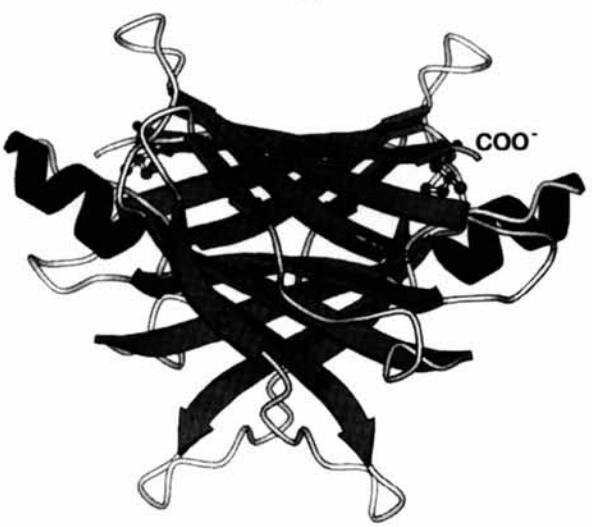

(*b*)

Fig. 1. (*a*) The stereographic representation of the mutant TTR tetramer viewed along the thyroxin binding channel. (*b*) The dimer subunit. Strands *A* to *H* forming the *DAGH* and *CBEF* sheets are indicated for one monomer; the position of Ile122 is shown for both monomers.

Table 1. *Summary of crystallographic information*

No. of unique reflections	19566
R_{merge} (%)	7.2
Overall completeness (%)	96
Space group	$P2_12_12$
a (Å)	43.2
b (Å)	85.6
c (Å)	65.5
Resolution (Å)	10.0–1.9
R value (%)	15.8
R.m.s. deviation in 1–2 bonded distances (Å)	0.019
R.m.s. deviation in 1–3 bonded distances (Å)	0.027

2. Experimental procedures

2.1. *Crystallization*

Recombinant TTR Ile122 was produced and purified as described by Furuya and co-workers (Furuya *et al.*, 1991). Crystals were grown at room temperature using the hanging-drop vapour-diffusion method. The drops contained equal volumes of 10 mg ml^{-1} protein solution and the reservoir solution composed of 41% ammonium sulfate, 200 m*M* sodium citrate, pH 5.3. Crystals with approximate dimensions of 0.2 × 0.2 × 0.2 mm grew in one month.

2.2. *Data collection and data processing*

The X-ray diffraction data to 1.9 Å resolution were collected at 287 K using synchrotron radiation on the X11 beamline at EMBL Hamburg. Two data sets, low and high resolution were collected on the same crystal. The low-resolution data set was collected to insure measurement of strong reflections overloaded in the high-resolution data set. The data were processed with *DENZO* (Otwinowski, 1993). A summary of the crystallographic information is given in Table 1.

2.3. *Structure determination and refinement*

Crystallographic refinement was carried out with the *CCP*4 (Collaborative Computational Project, Number 4, 1994) version of *PROLSQ* (Konnert & Hendrickson, 1980) and *ARP* (Lamzin & Wilson, 1993). The Fourier syntheses were calculated using the *CCP*4 package (Collaborative Computational Project, Number 4, 1994) and were visualized using *FRODO* (Jones, 1978). The initial model was that of wild-type TTR refined to an R factor of 17% at 1.7 Å resolution (Hamilton *et al.*, 1993). Seven rounds of positional and B-factor refinement coupled with manual rebuilding continued until the R factor converged. In each round of refinement new solvent molecules were automatically selected from peaks which appeared in the difference Fourier maps and made reasonable hydrogen bonds with protein atoms, while others were rejected because they were too close to the new peaks. All solvent molecules were assigned occupancies of 1.0. The substitution of valine by isoleucine at position 122 was clear from the maps. The final refined model has a crystallographic R factor of 15.8% and consists of 232 amino acids and 168 solvent molecules.

3. Results and discussion

3.1. *The quality of the model*

Out of a total of 254 amino acids in the dimer, composed of monomers A and B, the model consists of two continuous chains of 116 residues each. The N- and C-terminal residues are disordered and not defined in the electron density. Similar disorder was reported for the wild-type TTR (Hamilton *et al.*, 1992). For residues Cys10 to Ala125 the $3F_o - 2F_c$ density of the protein backbone is continuous in both monomers. A few flexible loops have, however, poorly defined electron density and refined to high temperature factors, reflecting a high mobility. Some side chains at the surface are also defined weakly.

The r.m.s. deviation from ideality in bond distances is 0.019 Å and in angle-bonded distances 0.027 Å. The overall R factor is 15.8% for all reflections between 10 and 1.9 Å resolution. The overall average temperature factor for the protein atoms is 23.5 Å^2 (18.6 for main-chain atoms and 28.7 for side-chain atoms). The positional error for all the atoms is 0.18 Å as estimated from σ_A plot (Read, 1986). The Ramachandran plot calculated using *PROCHECK* (Morris, MacArthur, Hutchinson & Thornton, 1992) showed no residues with main-chain dihedral angles in disallowed regions (Fig. 2). 91% of the residues are in the core regions.

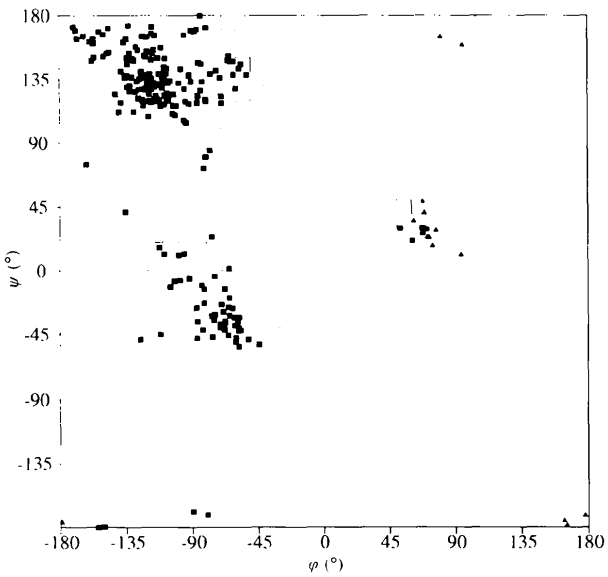

Fig. 2. Ramachandran plot for the final model. Glycine residues are shown as triangles.

Table 2. *Hydrogen bonds (Å) between main-chain atoms involved in the interaction of monomer (A) with monomer (B) of the dimer*

	Val122Ile mutant	Wild-type TTR
Tyr114 CO (*A*)···HN Ala120 (*B*)	2.95	3.02
Tyr114 CO (*B*)···HN Ala120 (*A*)	3.12	3.02
Tyr116 NH (*A*)···OC Thr118 (*B*)	3.08	3.11
Tyr116 NH (*B*)···OC Thr118 (*A*)	3.11	3.02
Tyr116 CO (*A*)···HN Thr118 (*B*)	2.92	2.94
Tyr116 CO (*B*)···HN Thr118 (*A*)	3.02	2.89
Glu89 NH (*A*)···OC Val94 (*B*)	2.86	2.84
Glu89 NH (*B*)···OC Val94 (*A*)	2.96	2.82

3.2. *Comparison with the wild-type structure*

Fig. 3 shows the electron-density map around position 122 before isoleucine was included in the model. In both monomers, a large bulb of density indicates the Val/Ile replacement. The substitution results in a small alteration of the adjacent polypeptide in order to accommodate the larger side chain.

TTR is a tetrameric protein. Each monomer is composed of two four-stranded antiparallel β-sheets, packed together, and hydrogen bonds between the two monomers result again in two β-sheets, each of them with eight strands. Only one dimer is present in the crystallographic asymmetric unit (Fig. 1*b*). The two dimers pack around a well defined channel where are located two thyroxin binding sites.

A displacement between the β-sheets in the dimer was described for the Val30Met TTR variant (Hamilton *et al.*, 1992). The authors suggested that this might affect the stability of the protein. We started our analysis of the three-dimensional structure of the protein by comparing the distances between residues in both sheets of the same dimer, in the case of TTR Ile122 and the wild-type protein. We observed that these distances were maintained in the variant protein.

Before calculating relative coordinate shifts of corresponding atoms in TTR Ile122 and wild-type TTR, unit-cell identity was considered and mutant coordinates were transformed into fractional and then back to orthogonal coordinates in the wild-type unit cell. The r.m.s. deviation between the CA positions of TTR Ile122 and TTR is 0.17 Å and the largest deviations correspond to residues 20–24, 37–39, 79–84, 100–104 and 122–125 from monomer *A* and 36–38, 77–86, 96–104 and 122–124 from monomer *B*. Apart from the residues 96–104 in monomer *B*, all the mentioned residues have deviations that are nearly twice the r.m.s. These residues belong to surface loops or to the region near the mutation, which is located near the C terminus.

Fig. 4 shows the average main-chain thermal parameters (*B*) for both monomers in TTR Ile122 and wild-type TTR.

Table 3. *Hydrogen bonds (Å) involved in dimer–dimer interactions*

Sym means symmetry-related dimer.

	Val122Ile mutant	Wild-type TTR
Gly22 CO (*A*)···HN Val122 sym	2.96	2.98
Gly22 CO (*B*)···HN Val122 sym	2.80	2.85
Ala19 CO (*A*)···HN Tyr114 sym	3.10	2.94
Ala19 CO (*B*)···HN Tyr114 sym	3.06	2.92

3.3. *The monomer–monomer contacts*

The principal contacts between monomers within a dimer correspond to hydrogen bonds between strands *F* and *F'* and *H* and *H'*, where *F* and *H* correspond, respectively, to residues His90–Asn98 and Tyr114–Ile122 of monomer *A*, and *F'* and *H'* correspond to the same residues in the monomer *B*. The hydrogen bonds between main-chain atoms involved in monomer–monomer interactions for the Val122Ile mutant and wild-type TTR are listed in Table 2. The monomer–monomer interactions are not affected in the crystal structure of the mutant protein.

3.4. *The dimer–dimer contacts*

Residue Ile122 is located at the edge of strand *H* is hydrogen bonded to strand *H'* from the other monomer in the dimer. It is one of the residues involved in dimer–dimer interactions, as shown in Table 3. The Val/Ile substitution causes a small alteration in the polypeptide chain. The cavity where residue Ile122 is located has hydrophobic interactions with residues Arg103 and Tyr105 from the same monomer and residues Phe87 and Tyr114 from the other monomer in the same dimer (Fig. 3). Residues Tyr105 and Tyr114 are important in maintaining the tertiary structure of the protein (Blake *et al.*, 1978). Tyr105 OH forms a hydrogen with Asn98 N. Tyr114 OH forms a water-bridged linkage with Pro86 O. In this way these residues are responsible for the stabilization of two loop regions in the monomer. When Ile replaces Val at position 122, besides the movement of the main-chain containing this residue, it is also observed that the side chain of Tyr114 in monomer *A* moves slightly and it no longer links to Pro86. This may result in a destabilization of the tertiary structure of the protein.

The dimer–dimer contacts, between main-chain atoms, result from residues located at the edges of the two β-sheets present in each dimer. The hydrogen-bond lengths involved in these interactions are given in Table 3 for both mutant and wild-type TTR. The values are not very different from those present in the wild-type

protein, although a small increase in the hydrogen bonds involving residues Ala19 and Tyr114 is noticed.

3.5. *Estimation of coordinate errors*

The estimation of coordinate error for TTR Ile122 obtained from the σ_A plot (Read, 1986) is 0.18 Å. This is the average accuracy for all atoms in the unit cell including both protein and solvent. The coordinate error for main-chain atoms, which are typically better defined, is expected to be lower.

The presence of two crystallographically independent monomers in the asymmetric unit allows the estimation of coordinate error by superposition of these molecules. The r.m.s. deviation between them would reflect: (1) the actual coordinate error as a function of both atomic temperature factor and resolution of the data. The latter means that an atom with zero temperature factor has non-zero error in its coordinates. (2) Crystal lattice contacts, which will effectively increase the determined coordinate error.

The CA atoms from the two monomers were superimposed. Large deviations for regions Ala36–Asp38, Gly83–Ser84, Ala97–Arg104 and C-terminal residues Thr123–Pro125 were observed. These arise from crystal lattice contacts. These regions were omitted and the superposition was repeated using 396 main-chain atoms of the remaining 99 residues. The r.m.s. deviation was 0.22 Å. The coordinate error for these atoms, therefore, becomes $0.22/2^{1/2} = 0.16$ Å, which is less than that derived from σ_A plot for all atoms in the unit cell. However, the value of 0.16 Å is likely to be overestimated as crystal contacts, though to a lesser extent, may still affect the positions of atoms used for comparison.

The r.m.s. deviation as a function of atomic temperature factors is shown in Fig. 5. Although the dependence was not expected to be linear (Rypniewski *et al.*, 1995), the straight line, nicely fitting the points is also given. Extrapolation to zero temperature factor gives a r.m.s. deviation (r.m.s.d.) of 0.07 Å, the value deemed to be achieved in the absence of atomic thermal motion.

Main-chain atoms of residues involved in the interdomain contacts have average temperature factors of about 9, 11, 9 and 22 Å^2 for Ala19, Gly22, Tyr114 and Ile122, respectively. The coordinate error is derived as r.m.s.d./$2^{1/2}$; from Fig. 5 the r.m.s.d.

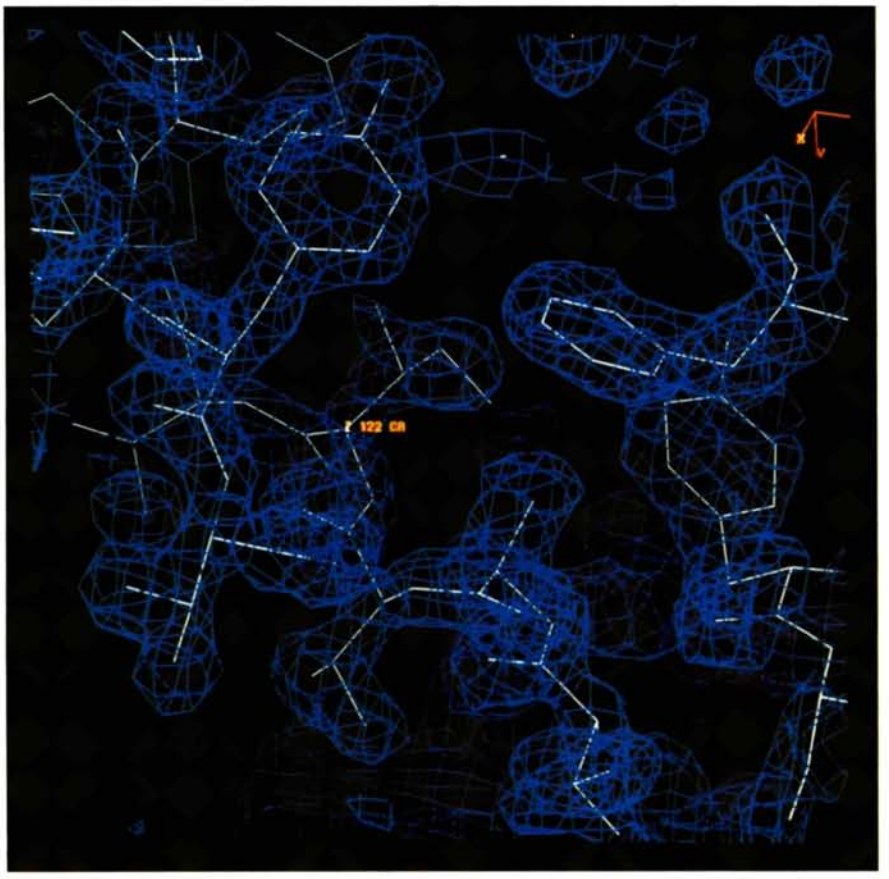

Fig. 3. $3F_o - 2F_c$ electron-density map calculated around residue Ile122.

values are 0.15, 0.17, 0.15 and 0.22 Å for Ala19, Gly22, Tyr114 and Ile122, respectively. The corresponding coordinate errors are: 0.11, 0.12, 0.11 and 0.16 Å. Thus, the accuracy in hydrogen bonds becomes $(0.11^2 + 0.11^2)^{1/2} = 0.15$ Å for the Ala19···Tyr114 hydrogen bond and $(0.12^2 + 0.16^2)^{1/2} = 0.2$ Å for the Gly22···Ile122 hydrogen bond. As pointed out above, superposition of crystallographically independent molecules gives overestimated values for coordinate error, the real errors are somewhat smaller. According to these calculations the values presented in Table 3 indicate that the difference in the Ala19···Tyr114 contact might just be significant, which would account for the destabilization of the tetrameric structure. In fact, Altland & Winter (1996), using an electrophoretic procedure, demonstrated that the tetramer stability in mutant TTR Ile122 is affected.

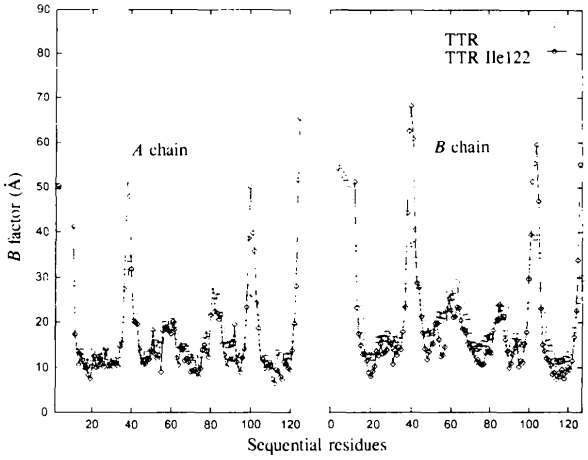

Fig. 4. The average main-chain thermal parameters (*B*) for both monomers in mutant and wild-type TTR.

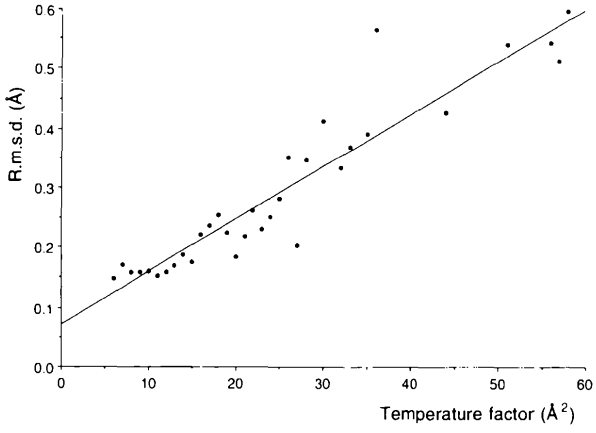

Fig. 5. Average r.m.s. deviation between main-chain atoms of the two crystallographically independent TTR monomers as a function of atomic temperature factors. 396 pairs of main-chain atoms were used for superposition and were sorted according to their temperature factors. Average r.m.s. deviation was calculated for each temperature-factor shell.

4. Conclusions

More than 40 amyloidogenic TTR mutations have been described in the literature (Saraiva, 1995). The mechanism involved in the deposition of the protein is not known but it has been shown that it is possible to form amyloid fibrils when the protein is in its monomeric form (Westermark, Sletten, Johansson & Cornwell, 1990; Kelly & Lasbury, 1994). This is consistent with a variation in the protein stability, which might result from a conformational modification.

In our study we concluded that the overall structures of Val122Ile mutant and wild-type TTR are essentially identical. However, there are small changes in the region associated with the intra- and interdimer interactions which may lead to a destabilization of the tetrameric form of the protein. Higher resolution crystal structure analysis is required to obtain more detailed information about small alterations between the wild-type and the variant structures.*

We thank Dr Z. Dauter for helpful discussion. The research was supported by EU BIOMED programme No. BMH1-CT92-1076, HCMP programme No. CHRX-CT93-0143 and EU LIP programme. We thank the European Union for support of the work at EMBL Hamburg through the HCMP Access to Large Installation Project, contract number CHGE-CT93-0040.

* Atomic coordinates and structure factors have been deposited with the Protein Data Bank, Brookhaven National Laboratory (Reference: 1TTR, R1TTRSF). Free copies may be obtained through The Managing Editor, International Union of Crystallography, 5 Abbey Square, Chester CH1 2HU, England (Reference: LI0221).

References

Altland, K. & Winter, P. (1996). *Electrophoresis*. In the press.

Andrade, C. (1952). *Brain*, **75**, 408–427.

Andrade, C., Arakis, A. & Block, W. D. (1970). *Arthritis Rheum.* **13**, 902–915.

Blake, C. C. F., Geisow, M., Oatley, S., Rerat, B. & Rerat, C. (1978). *J. Mol. Biol.* **121**, 339–356.

Collaborative Computational Project, Number 4. (1994). *Acta Cryst.* D**50**, 760–763.

Damas, A. M., Terry, C. J. & Blake, C. C. F. (1990). *Arq. Med.* **3**, 55–57.

Damas, A. M., Terry, C. J., Blake, C. C., Palha, J., Matias, P., Saraiva, M. J. & Sakaki, Y. (1993). *J. Rheumatol.* **20**, 727.

Furuya, H., Saraiva, M. J. M., Gawinowicz, M., Alves, I., Costa, P. P., Sasaki, H., Goto, I. & Sakaki, Y. (1991). *Biochemistry*, **30**, 2415–2421.

Gorevic, P., Prelli, F., Wright, J., Pras, M. & Frangione, B. (1989). *J. Clin. Invest.* **83**, 836–843.

Hamilton, J. A., Steinrauf, L. K., Braden, B. C., Liepnieks, J., Benson, M., Holmgren, G., Sandgren, O. & Steen, L. (1993). *J. Biol. Chem.* **268**, 2416–2424.

Hamilton, J. A., Steinrauf, L. K., Liepnieks, J., Benson, M., Holmgren, G., Sandgren, O. & Steen, L. (1992). *Biochim. Biophys. Acta*, **1139**, 9–16.

Jones, T. A. (1978). *J. Appl. Cryst.* **11**, 268–272.

Kelly, J. W. & Lasbury, P. T. (1994). *Amyloid Int. J. Exp. Clin. Invest.* **1**, 186–205.

Konnert, J. H. & Hendrickson, W. A. (1980). *Acta Cryst.* A**36**, 344–350.

Lamzin, V. S. & Wilson, K. S. (1993). *Acta Cryst.* D**49**, 129–147.

Monaco, H. L., Rizzi, M. & Coda, A. (1995). *Science*, **268**, 1039–1041.

Morris, A. L., MacArthur, M. W., Hutchinson, E. G. & Thornton, J. M. (1992). *Proteins*, **12**, 345–364.

Otwinowski, Z. (1993). *DENZO: An Oscillation Data Processing Program for Macromolecular Crystallography*. Yale University, New Haven, CT, USA.

Read, R. J. (1986). *Acta Cryst.* A**42**, 140–149.

Rypniewski, W. R., Mangani, S., Bruni, B., Orioli, P. L., Casati, M. & Wilson, K. S. (1995). *J. Mol. Biol.* **251**, 282–296.

Saraiva, M. J. M. (1991). *Neurom. Disorders*, **1**, 3–6.

Saraiva, M. J. M. (1995). *Hum. Mutat.* **5**, 191–195.

Saraiva, M. J. M., Birken, S., Costa, P. P. & Goodman, D. S. (1984). *J. Clin. Invest.* **74**, 104–119.

Terry, C., Damas, A. M., Oliveira, P., Saraiva, M., Alves, I., Costa, P., Sakaki, Y. & Blake, C. (1993). *EMBO J.* **12**, 735–741.

Westermark, P., Sletten, K., Johansson, B. & Cornwell, M. G. (1990). *Proc. Natl Acad. Sci. USA*, **87**, 2843–2845.